Integrating Long-term Optogenetic Stimulation and Bioluminescence Recording to Study Neural Plasticity Induced by Circadian Entrainment

Authors:

Suil Kim[1] and Douglas G. McMahon*[1,2]

Author Affiliations:

[1]Vanderbilt Brain Institute, Vanderbilt University, Nashville, TN, USA

[2]Department of Biological Sciences, Vanderbilt University, Nashville, TN, USA

*Correspondence to: douglas.g.mcmahon@vanderbilt.edu

Abstract

Entrainment of the suprachiasmatic nucleus (SCN) circadian clock in the brain to environmental light cycles is a form of neural plasticity which involves acute daily clock resetting, and long-term changes in endogenous clock period. Elucidating mechanisms of entrainment is critical for understanding how circadian clocks maintain alignment of internal rhythms with the external environment. However, studying how the SCN clock *per se* behaves throughout entrainment at the molecular level remains technically challenging. Here we report a novel experimental system that precisely employs periodic optogenetic stimulation to drive circadian entrainment of multiple SCN brain slices while recording circadian rhythms in molecular output with bioluminescence. Using this system, we demonstrate entrainment of the SCN clock *ex vivo* and show that many forms of circadian clock plasticity in behavior is intrinsic to the SCN molecular clock plasticity induced through encoding different light cycle periods and seasonal variations in the day length.

Introduction

In response to recurring stimuli, neurons and networks encode and enact enduring changes in neural function and behavior. Understanding such neural plasticity is crucial to advancing knowledge of how neural networks and systems of the brain adapt to and represent previous experience. The mammalian brain's 24-hour timing mechanism, or the circadian clock, is a system well-suited for studying molecular mechanisms of neural plasticity in that the central clock—the suprachiasmatic nucleus (SCN) of the hypothalamus—is a highly localized neural network that is sufficient and necessary for driving circadian behavior [1–3]. The SCN retains its clock function when isolated and thus can be employed to explore molecular, cellular, and circuit mechanisms underlying circadian behavior in a setting more accessible to manipulation. Entrainment (i.e., the coupling of an endogenous circadian rhythm to an environmental rhythm) of the SCN clock to environmental light cycles via retinal projections is a cardinal example of neural plasticity, and shares mechanistic elements with long-term synaptic plasticity[4]. Further understanding mechanisms of entrainment is critical for revealing how circadian clocks maintain alignment of internal rhythms with the external environment. However, experimentally inducing light entrainment and SCN plasticity *ex vivo* has been very challenging, as it requires periodic stimulation for multiple days with good temporal precision to repeatedly reset the circadian clockworks.

Here we have developed a novel experimental system that precisely employs periodic optogenetic stimulation to enable entrainment of multiple SCN brain slices while recording circadian rhythms in molecular output with bioluminescence. Using this system, we demonstrate entrainment of the SCN clock *ex vivo* and provide insights into SCN clock plasticity resulting from encoding different light cycle periods and seasonal variations in the day length.

Results

An integrated system for long-term optogenetic stimulation and bioluminescence recording

To entrain the SCN slice with optogenetic stimulation, light pulses must be given periodically for multiple days. While optogenetics using channelrhodopsin-2 (ChR2) has been used to successfully entrain circadian rhythms *in vivo*[5], long-term blue light exposure in culture can decrease cell viability via toxic byproducts[6] and can alter gene expression including neuronal activity-regulated genes[7]. To test the effects of sustained blue light exposure on SCN slices, we delivered blue light pulses (470nm, 10Hz frequency, 10ms width, 1.2mW/mm^2) for 12h to SCN expressing a bioluminescent reporter of the core clock gene *Per2*, PER2::LUC[8], but no optogenetic construct. We found that PER2::LUC bioluminescence became arrhythmic following the prolonged blue light exposure (Fig. 1a-b). This effect was not reversible with a medium change (Fig. 1a), suggesting that long-term blue light exposure *per se* can elicit photodynamic damage to the SCN tissue in isolated culture.

Since phototoxicity decreases with increasing irradiation wavelength[7,9], we tested whether using red light (625nm) mitigates the phototoxicity. 12h red light pulses (625nm, 10Hz, 10ms, 1.25mW/mm^2) did not significantly affect the PER2::LUC rhythm in SCN slices (Fig. 1a-b), suggesting that using red light stimulation is more feasible for prolonged optogenetic light stimulation *ex vivo*. We thus expressed a red light-activated opsin, ChrimsonR[10], in SCN slices using AAVs (Fig. 1c).

To extend the duration over which we can observe the SCN slice throughout entrainment, we improved the quality and robustness of PER2::LUC rhythmicity by using brain slices from younger mice that usually survive longer in culture[11], and stabilized glutamine media that helps reduce toxic ammonia byproduct in culture[12,13] (Supplemental Fig. 1). For precise temporal control of optogenetic stimulation of multiple SCN slices, we integrated an optogenetic stimulation apparatus into a multi-channel luminometer (Fig.

1d). To minimize the potential effect of LED-generated heat on SCN rhythmicity while achieving sufficient light intensity for optogenetic stimulation, we set up a light delivery path in which an LED placed outside the incubator housing the luminometer delivered 625nm light through a fiber optic cable and a collimation lens (Fig. 1d). We then created a program interface for remotely operating PER2::LUC luminometry and optogenetic stimulation in a coordinated manner (Supplementary Fig. 2).

To characterize how this integrated system induces phase resetting of circadian rhythms that fundamentally underlies circadian entrainment, we applied single optogenetic light stimulations to SCN slices at three different circadian times (CT) as defined by the timing of the intrinsic PER2::LUC rhythm of each SCN slice. By convention, CT12 was defined as the peak time of the PER2::LUC rhythm and is correlated *in vivo* with the onset of nocturnal behavioral activity[8]. Thus, the rising phase of the PER2::LUC rhythm represents the day phase of intrinsic SCN circadian time, while the falling phase corresponds to physiological night. Light stimulation *in vivo* at CT6, CT14, and CT21 induces representative phase responses in the locomotor circadian rhythm (no phase shift, phase delays, and phase advances, respectively)[14,15]. We found that the phase responses to optogenetic light stimulation *ex vivo* indeed mimicked the responses to the light stimulations *in vivo* (Fig. 2a-b). Optogenetic stimulation of the *ex vivo* SCN at CT6 induced no phase shifts whereas the optogenetic stimulation at CT14 and CT21 induced phase delays and phase advances of about 4hr, respectively (Fig. 2b), similar to phase responses observed to ChR2[5]. Notably, these acute phase shifts were accompanied by a change in the free-running circadian period (i.e., circadian period of an oscillator in the absence of external time cues such as light) of the SCN clock that persisted for several days as an after-effect of the acute phase shifting stimulations (Fig. 2a, c). Similar to *in vivo*[16], phase delays led to period lengthening on subsequent cycles whereas phase advances resulted in period shortening (Fig. 2c). Taken together, an

integrated system of PER2::LUC luminometry and ChrimsonR optogenetic stimulation can induce phase resets in the *ex vivo* SCN clock that mimic light-induced circadian phase resetting *in vivo*.

Entrainment of the SCN clock *ex vivo* to different T-cycles

Individual phase shifts by external time cues are the building blocks of circadian entrainment[17]. Daily, repeated phase shifts to light adjust the endogenous period of the circadian clock to the match the 24-hour solar day and align circadian rhythms in a particular temporal relationship with the daily light-dark cycle (i.e., phase angle of entrainment). To test whether optogenetic stimulation can entrain the isolated SCN clock, we delivered periodic optogenetic light stimuli (625nm, 10Hz, 10ms, 1.25mW/mm^2) at intervals (optogenetic day-lengths, or T-cycles) that significantly deviated from the near 24-hour endogenous period of the SCN to clearly differentiate the entrained state from free-running. One cohort of slices (T22) was stimulated every 22h while the other cohort (T25) was stimulated every 25h (Fig. 3a). SCN in both cohorts demonstrated the classic conditions defining circadian entrainment—matching of clock period to the period of the input stimulus (Fig. 3b), adopting a stable timing relationship with the repeating stimulus (stable phase angle, Fig. 3c), and initiating a subsequent free-run from the point in time of the entrained phase angle upon cessation of the stimulus (Fig. 3a). Importantly, the SCN molecular clock entrained to the different T cycles with different phase angles of entrainment (Fig. 3c), as predicted by non-parametric model of circadian entrainment, and observed *in vivo*[17]. SCN exposed to optogenetic T22 reached stable entrainment with the periodic optogenetic stimulation aligned near the trough of the PER2::LUC rhythm, where single stimuli produced phase advances, while those exposed to optogenetic T25 cycles entrained with stimulation aligned near the peak of the rhythm, where single stimuli produced phase delays (Fig. 3a).

In addition, optogenetic entrainment of the isolated SCN also induced clock plasticity in the form of after-effects on the free-running period. Surprisingly, however, the period after-effects of the repeated phase shifts mediating entrainment were less consistent and smaller in amplitude than those of single phase shifts. Entrainment to long T cycles showed a trend in subsequently lengthening the SCN molecular clock period, similar to the period plasticity induced by *in vivo* T-cycle entrainment and behavioral rhythms[16], but it did not reach statistical significance (Fig. 3d).

Entrainment of the SCN clock *ex vivo* to skeleton photoperiods

Circadian oscillators in the SCN encode the length and timing of the daily light period (i.e., photoperiod)[18,19], thereby promoting seasonal changes in physiology and behavior. Strikingly, light cycles consisting of brief light pulses only defining dawn and dusk (i.e., skeleton photoperiods) can simulate most aspects of full photoperiods at the behavioral level, as if the interval between the dawn and dusk pulses is treated as a complete light phase[17]. Thus, it has been hypothesized that the SCN clock itself is entrained to different photoperiods primarily by the daily light transitions at dawn and dusk, although this has not been tested directly.

To test how the isolated SCN clock entrains to different photoperiods, we applied to SCN slices an optogenetic equivalent of skeleton photoperiods mimicking short (winter-like), equinox, or long (summer-like) photoperiods (8h, 12h, and 16h daylight per day), respectively. For the 12:12 skeleton photoperiod entrainment, we gave short optogenetic stimulations (15 min) twice per day (12h apart), initiated with one stimulation aligned near the trough of the free-running PER2::LUC rhythm to mimic dawn, and the other stimulation aligned near the peak to mimic dusk of the free-running PER2::LUC rhythm before entrainment (Fig. 4a). The 12:12 skeleton indeed entrained SCN slices such that the

circadian period of the SCN molecular rhythms during entrainment became matched to the 24h optogenetic light cycle length, and the phase angle of entrainment (measured as the difference in time between the dusk pulse and the half-max on the rising phase of PER2::LUC rhythm) was stable (Fig. 4a-b). To test for 8:16 short day skeleton photoperiod entrainment, we gave twice-daily optogenetic stimulations 8h apart, with the "dawn" pulse initially aligned near the trough of the free-running PER2::LUC rhythm, and the "dusk" pulse initially aligned near the peak (Fig. 4a). The 8:16 short skeleton photoperiod entrainment rapidly produced a stable phase relationship between the PER2::LUC rhythm and the nominal dusk pulse such that the rising phase (SCN day) was encompassed within the 8h "short day" interval (Fig. 4a-b). To test for entrainment to 16:8 long day skeleton photoperiods, we gave optogenetic stimulations twice daily 16h apart, with the "dawn" and "dusk" pulses initially encompassing the rising phase of the PER2::LUC rhythm within the 16h "day". However, SCN slices in this 16:8 long cohort did not stably align within the 16h "long day" interval, but instead rapidly phase-advanced across the nominal dawn pulse to stably entrain with the rising phase of the PER2::LUC rhythms (SCN day) within the short 8hr interval at similar phase angles to the short day cohort – effectively exhibiting a bias toward short day entrainment (Fig. 4a-b). Remarkably, this phenomenon of "phase jumping" across skeleton photoperiods to entrain to the shorter interval is a long-established property of behavioral entrainment in both mice and flies[17] (Supplementary Fig. 3), the basis of which is not well understood. Our data suggests that the behavioral preference in mice toward entrainment to shorter cycle intervals as the day phase resides within the SCN itself.

In addition, entrainment to different skeleton photoperiods also altered the molecular waveform of the SCN clock. Optogenetic pulses at dawn phase-advanced the PER2::LUC rhythm and increased the maximum slope of the rising phase whereas the pulses at dusk delayed the end of the cycle (Fig. 4e, Supplemental Fig. 4). The net effect was that the rising phase relative to the falling phase became

shorter than before entrainment (Fig. 4f). However, changes in the waveform were not sustained in constant darkness after entrainment (Fig. 4e-f), suggesting that the waveform changes are direct effects of optogenetic light stimulation accelerating and decelerating different phases of the molecular clock during entrainment. As *in vivo*[17], finally, entrainment to the 8:16 skeleton photoperiods induced a trend toward circadian period lengthening as an after-effect, although these did not reach statistical significance. Taken together, applying optogenetic skeleton photoperiods to SCN slices recapitulates skeleton photoperiod entrainment and induced plasticity in animals.

Conclusions

Our results demonstrate the ability to induce in the *ex vivo* SCN neural network the critical process of entrainment, whereby the core clock is synchronized to external time. Our method enables *ex vivo* manipulation of the isolated SCN over intervals of days to weeks, similar to entrainment stimuli *in vivo*, and evokes plasticity in the SCN clockworks that mirrors *in vivo* behavioral plasticity to entraining stimuli. The key advantages of our system for the study of long-term neural plasticity in isolated neural networks are the use of ChrimsonR opsin and red light to limit photodynamic damage from repeated stimulation, improved culture techniques, and automation of periodic optogenetic stimulation during bioluminescence recording, which combine to greatly extend the duration over which we can stimulate and record experimental data.

Our studies have revealed novel insights into plasticity of the mammalian central circadian clock. Although the SCN receives both extensive feed-forward and feedback from other brain nuclei *in situ*[20], we found that many of the classically studied forms of circadian plasticity and properties of entrainment apparently reside intrinsically within the SCN neural network itself. Interestingly, the characteristic

phase-dependence of phase resetting behavior – delays in the early circadian night, advances in in the late circadian night, and a "dead zone" in the mid-day where light does not reset the clock – is evident even though we stimulated SCN neurons directly, rather than them receiving retinal input. Thus, the mechanisms that determine the circadian phase response curve are intrinsic to the SCN, as also suggested for the phase response of molluscan circadian clock neurons to direct current injection[21]. Further, we found that SCN itself can indeed be entrained directly by the transitions in skeleton photoperiods as mimicked by optogenetic stimulation, and higher order aspects of entrainment, such as the bias of the circadian system to resolve ambiguous skeleton light cycles in favor of short-day entrainment[17], also resides in the SCN clockworks.

In addition, the long-term plasticity in clock period following phase shifts or entrainment is intrinsic to the SCN itself. This has been hypothesized based on classic *in vivo* studies of behavioral after-effects following phase shifts or entrainment[16], and we now demonstrate this directly. Importantly, a number of studies have suggested that SCN period plasticity in response to genetic or environmental perturbations also can be influenced by extra-SCN brain regions[22–25]. Our method enables differentiation and study of the SCN-intrinsic mechanisms of plasticity. Moving forward, our system now provides an enhanced basis to study mechanisms of intrinsic plasticity in the mammalian central circadian clock, including for example, regulation of gene expression in the molecular clockworks through DNA-methylation[23,26].

Our system can also be adapted for long-term optogenetic stimulation with bioluminescence-based Ca^{2+} indicators, such as bioluminescence resonance energy transfer (BRET) Ca^{2+} sensors[27,28], and thus it is potentially widely applicable to studying induction of long-term neural plasticity in different regions of the brain.

Methods

Animals and Housing

P11-14 heterozygous PER2::LUC knock-in mice[8] were used for organotypic slice culture and subsequent procedures. All animals were housed in a 12:12 LD cycle, and had food and water provided ad libitum. Experiments were performed in accordance with the Vanderbilt University Institutional Animal Care and Use Committee and National Institutes of Health guidelines.

Organotypic slice culture and AAV viral transduction

Removed brains were mounted and cut into coronal slices (300µm) on a vibrating blade microtome (Leica) in cold HBSS supplemented with 100 U/ml penicillin/streptomycin, 10 mM HEPES, and 4.5 mM sodium bicarbonate. The SCN slices were dissected out and transferred onto a PTFE membrane insert (Millipore) in 35-mm culture dishes with 1.2 ml of DMEM (D5030, Sigma) supplemented with 3.5 g/L D-glucose, 0.2mM Glutamax (Gibco), 10 mM HEPES, 25 U/ml penicillin/streptomycin, 2% B-27 Plus (Gibco), and 0.1 mM D-Luciferin sodium salt (Tocris). The SCN slice position was adjusted to the center of the dish and 1.5µl AAV (pAAV1-Syn-ChrimsonR-tdT, Addgene) was placed directly onto the SCN slice. The culture dishes were then sealed with an optically clear PCR plate film (Bio-Rad) and maintained in a non-humidified incubator at 36.8 °C for about 10 days. pAAV1-Syn-ChrimsonR-tdT was a gift from Edward Boyden (Addgene plasmid # 59171)[2]. The opsin expression was checked after about 10 days of viral transduction by imaging tdT fluorescence.

Bioluminescence recording and in situ optogenetic stimulation

After viral transduction, bioluminescence from firefly luciferase in each of PER2::LUC SCN slices was recorded in 6 min intervals by a 32-channel/4-photomultiplier tube luminometer LumiCycle (Actimetrics) in a non-humidified, light-tight incubator at 36.8°C. Baseline rhythms were recorded for at

least three days before optogenetic stimulation. For optogenetic stimulation, 625nm LED light (10Hz, 10ms pulse width, 1.5mW/mm^2) was delivered at the center of a target culture dish by a fiber-coupled LED (M625F2, Thorlabs). The LED was located outside the incubator and coupled to a multimode fiber cable (Ø1500µm, 0.39NA) (M93L, Thorlabs) and a fiber collimation package (F230SMA-B, Thorlabs) tethered above samples. Light pulses were generated by an LED driver (LEDD1B, Thorlabs) and a signal generator (Mhinstek). For remotely turning on and off the photomultiplier tubes in the luminometer, a relay switch (DC60S5-B, Sensata-Crydom) was added in the electrical circuit of the luminometer and connected to a multi-functional I/O device (USB-6001, National Instruments). Custom-written code in Matlab (Mathworks) was used to access luminescence data collection software (Actimetrics), the multi-functional I/O device, and a signal generator software (Mhinstek). The Matlab code loaded a spreadsheet having stimulation settings and time schedules, and executed a series of events during optogenetic stimulation: pause bioluminescence recording, target positioning, stimulation initiation, stimulation termination, and resumption of the recording. For a long light exposure test, 12h blue or red light pulses (10Hz, 10ms pulse width, 1.2mW/ mm^2) were illuminated onto PER2::LUC SCN slices by LEDs (M470F3 or M625F2, respectively, Thorlabs) coupled to a multimode fiber cable (Ø1500µm, 0.39NA) (M93L, Thorlabs). Blue light-illuminated samples were given a medium change two days after illumination.

Bioluminescence data analysis and visualization

Raw bioluminescence data were baseline-subtracted using 24h running averages and smoothed by 2.4h moving averages using LumiCycle Analysis software (Actimetrics), and then they were loaded as normalized actograms into Matlab-run ClockLab software (Actimetrics) for further analyses. Phase shifts were determined as the time difference between the observed post-stimulation peak of the bioluminescence rhythm and the predicted peak from a linear regression of at least three cycles before

stimulation. Period changes were determined as the difference in the period length between the pre-stim and the post-stim cycles. Period length was calculated using a linear regression of at least three peaks. If peaks were not obvious, the period length was determined using half-maxes. For data visualization, smoothed and baseline-subtracted bioluminescence rhythms were represented as double-plotted actograms normalized to min and max values of the data for each line of the actograms, using Excel (Microsoft) and Prism (Graphpad). The actograms were 24h-plotted unless otherwise stated. Bioluminescence rhythms of 12h light-exposed slices were visualized using Excel (Microsoft) and LumiCycle Analysis software (Actimetrics). For quantifying the effect of a long light exposure on the rhythm amplitude, the amplitude of the first post-treatment cycle was normalized to the amplitude of the last pre-treatment cycle. For waveform analysis, the smoothed first derivatives were taken from the smoothed, baseline-subtracted bioluminescence rhythms normalized to min and max values, using Excel (Microsoft) and Prism (Graphpad). The duration of rising and falling phases was determined using the time duration between the zero crossings of the first derivatives. If the first derivatives were close to zero but did not make a zero crossing due to an increase immediately following an optogenetic stimulation, the local minimum was used as the end of the rising phase.

Statistical analysis

All statistical analyses (Student's *t*-test, One-Way ANOVA, Tukey's multiple comparisons test) were performed in Prism (Graphpad). Data are presented as a mean ± standard error of mean (SEM) and differences between groups were considered statistically significant when $p < 0.05$.

Acknowledgments:

This study was supported by NIH R01 GM117650 to D.G.M.

Author Contributions:

S.K. and D.G.M. conceived of the project. S.K performed the experiments. S.K and D.G.M. wrote the paper.

References

1. Moore, R. Y. & Eichler, V. B. Loss of a circadian adrenal corticosterone rhythm following suprachiasmatic lesions in the rat. *Brain Res.* **42**, 201–206 (1972).

2. Stephan, F. K. & Zucker, I. Circadian rhythms in drinking behavior and locomotor activity of rats are eliminated by hypothalamic lesions. *Proc. Natl. Acad. Sci. U. S. A.* **69**, 1583–1586 (1972).

3. Lehman, M. N. *et al.* Circadian rhythmicity restored by neural transplant. Immunocytochemical characterization of the graft and its integration with the host brain. *J. Neurosci.* **7**, 1626–1638 (1987).

4. Iyer, R., Wang, T. A. & Gillette, M. U. Circadian gating of neuronal functionality: A basis for iterative metaplasticity. *Frontiers in Systems Neuroscience* vol. 8 164 (2014).

5. Jones, J. R., Tackenberg, M. C. & McMahon, D. G. Manipulating circadian clock neuron firing rate resets molecular circadian rhythms and behavior. *Nat. Neurosci.* **18**, 1–5 (2015).

6. Stockley, J. H. *et al.* Surpassing light-induced cell damage in vitro with novel cell culture media. *Sci. Rep.* **7**, 1–11 (2017).

7. Tyssowski, K. M. & Gray, J. M. Blue light increases neuronal activity-regulated gene expression in the absence of optogenetic proteins. *eNeuro* **6**, 0085–19.2019 (2019).

8. Yoo, S. H. *et al.* PERIOD2::LUCIFERASE real-time reporting of circadian dynamics reveals persistent circadian oscillations in mouse peripheral tissues. *Proc. Natl. Acad. Sci. U. S. A.* **101**, 5339–5346 (2004).

9. Waldchen, S., Lehmann, J., Klein, T., Van De Linde, S. & Sauer, M. Light-induced cell damage in live-cell super-resolution microscopy. *Sci. Rep.* **5**, 1–12 (2015).

10. Klapoetke, N. C. *et al.* Independent optical excitation of distinct neural populations. *Nat. Methods* **11**, 338–346 (2014).

11. Humpel, C. Neuroscience forefront review organotypic brain slice cultures: A review. *Neuroscience* vol. 305 86–98 (2015).

12. Christie, A. & Butler, M. The adaptation of bhk cells to a non-ammoniagenic glutamate-based culture medium. *Biotechnol. Bioeng.* **64**, 298–309 (1999).

13. Imamoto, Y., Tanaka, H., Takahashi, K., Konno, Y. & Suzawa, T. Advantages of AlaGln as an additive to cell culture medium: Use with anti-CD20 chimeric antibody-producing POTELLIGENT™ CHO cell lines. *Cytotechnology* **65**, 135–143 (2013).

14. Daan, S. & Pittendrigh, C. S. A Functional analysis of circadian pacemakers in nocturnal rodents - II. The variability of phase response curves. *J. Comp. Physiol.* **106**, 253–266 (1976).

15. Johnson, C. H. Forty years of PRCs - What have we learned? *Chronobiology International* vol. 16 711–743 (1999).

16. Pittendrigh, C. S. & Daan, S. A functional analysis of circadian pacemakers in nocturnal rodents - I. The stability and lability of spontaneous frequency. *J. Comp. Physiol.* **106**, 223–252 (1976).

17. Pittendrigh, C. S. & Daan, S. A functional analysis of circadian pacemakers in nocturnal rodents - IV. Entrainment: Pacemaker as clock. *J. Comp. Physiol.* **106**, 291–331 (1976).

18. Rusak, B. & Morin, L. P. Testicular Responses to Photoperiod Are Blocked by Lesions of the Suprachiasmatic Nuclei in Golden Hamsters1. *Biol. Reprod.* **15**, 366–374 (1976).

19. Goldman, B. D. Mammalian Photoperiodic System: Formal Properties and Neuroendocrine Mechanisms of Photoperiodic Time Measurement. *J. Biol. Rhythms* **16**, 283–301 (2001).

20. Dibner, C., Schibler, U. & Albrecht, U. The Mammalian Circadian Timing System: Organization and Coordination of Central and Peripheral Clocks. *Annu. Rev. Physiol.* **72**, 517–549 (2010).

21. McMahon, D. G. & Block, G. D. The Bulla ocular circadian pacemaker - I. Pacemaker neuron membrane potential controls phase through a calcium-dependent mechanism. *J. Comp. Physiol.* **161**, 335–346 (1987).

22. Aton, S. J., Block, G. D., Tei, H., Yamazaki, S. & Herzog, E. D. Plasticity of circadian behavior and the suprachiasmatic nucleus following exposure to non-24-hour light cycles. *J. Biol. Rhythms* **19**, 198–207 (2004).

23. Azzi, A. *et al.* Network Dynamics Mediate Circadian Clock Plasticity. *Neuron* **93**, 441–450 (2017).

24. Ciarleglio, C. M., Resuehr, H. E. S., Axley, J. C., Deneris, E. S. & McMahon, D. G. Pet-1 Deficiency Alters the Circadian Clock and Its Temporal Organization of Behavior. *PLoS One* **9**, e97412 (2014).

25. Molyneux, P. C., Dahlgren, M. K. & Harrington, M. E. Circadian entrainment aftereffects in suprachiasmatic nuclei and peripheral tissues in vitro. *Brain Res.* **1228**, 127–134 (2008).

26. Azzi, A. *et al.* Circadian behavior is light-reprogrammed by plastic DNA methylation. *Nat. Neurosci.* **17**, 377–382 (2014).

27. Yang, J. *et al.* Coupling optogenetic stimulation with NanoLuc-based luminescence (BRET) Ca++ sensing. *Nat. Commun.* **7**, 1–10 (2016).

28. Suzuki, K. *et al.* Five colour variants of bright luminescent protein for real-time multicolour bioimaging. *Nat. Commun.* **7**, 1–10 (2016).

Figures

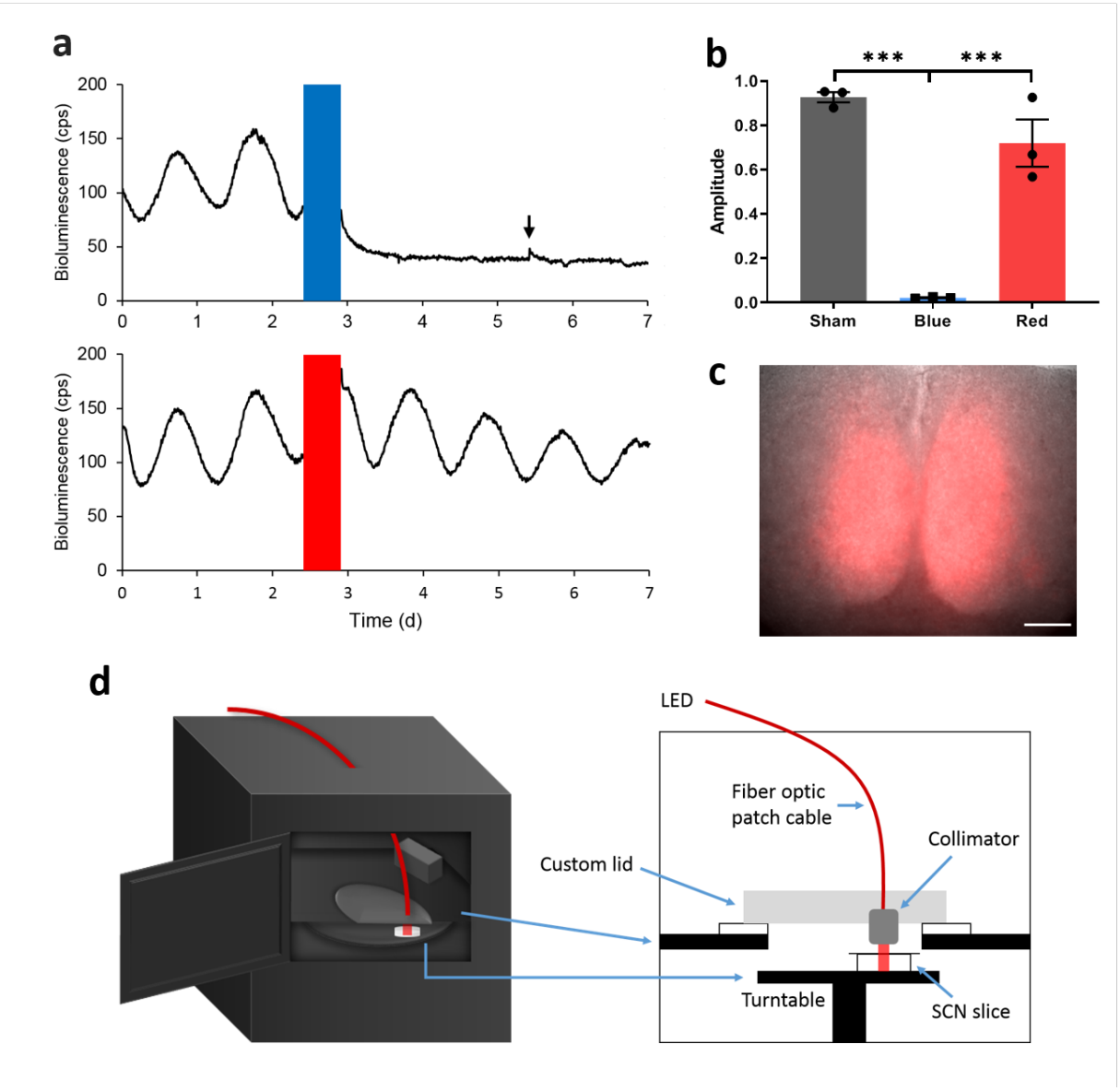

Fig. 1: Development of an integrated system of long-term optogenetic stimulation and bioluminescence recording. a Representative PER2::LUC bioluminescence rhythms of SCN slices exposed to either red (top) or blue (bottom) 10Hz light pulses (red or blue bars) for 12h. The black arrow indicates the timing of media change. **b** Fold change in the rhythm amplitude following sham, blue, or red light exposure (Student t-test, mean ± SEM, n = 3, ***$p < 0.001$). **c** Merged ChrimsonR-tdT fluorescence and the brightfield images of an SCN slice. Scale = 100µm. **d** Diagrams showing a multi-channel luminometer integrated with an optogenetic stimulation apparatus.

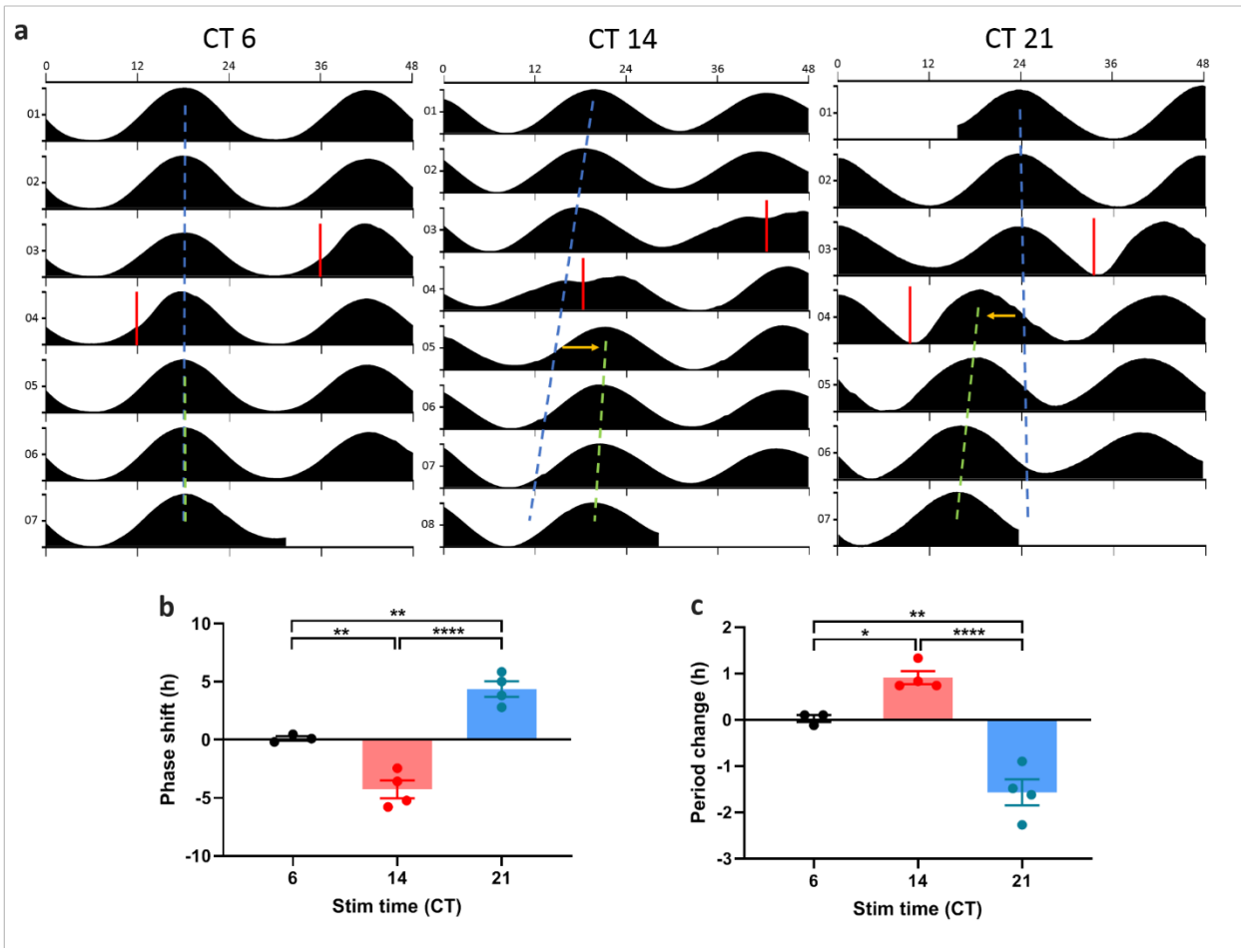

Fig. 2: ChrimsonR-driven optogenetic stimulation can reset the SCN clock. a Representative double-plotted PER2::LUC bioluminescence actograms of SCN slices stimulated with single 15m 10Hz optogenetic pulses (red bar) at circadian time (CT) 6 (left), 14 (middle), and 21 (right). Linear regressions of the pre-stimulation and post-stimulation cycle peaks are indicated as the blue and green dashed lines, respectively. Phase shifts are depicted by a yellow arrow. **b, c** Quantification of phase shifts (**b**) and period changes (**c**). Positive and negative phase shifts indicate phase advance and delay, respectively. Positive and negative period changes indicate period lengthening and shortening, respectively. (One-way ANOVA with Turkey's multiple comparisons test, mean ± SEM, n = 3-4, *p < 0.05, **p < 0.01, ****p < 0.0001).

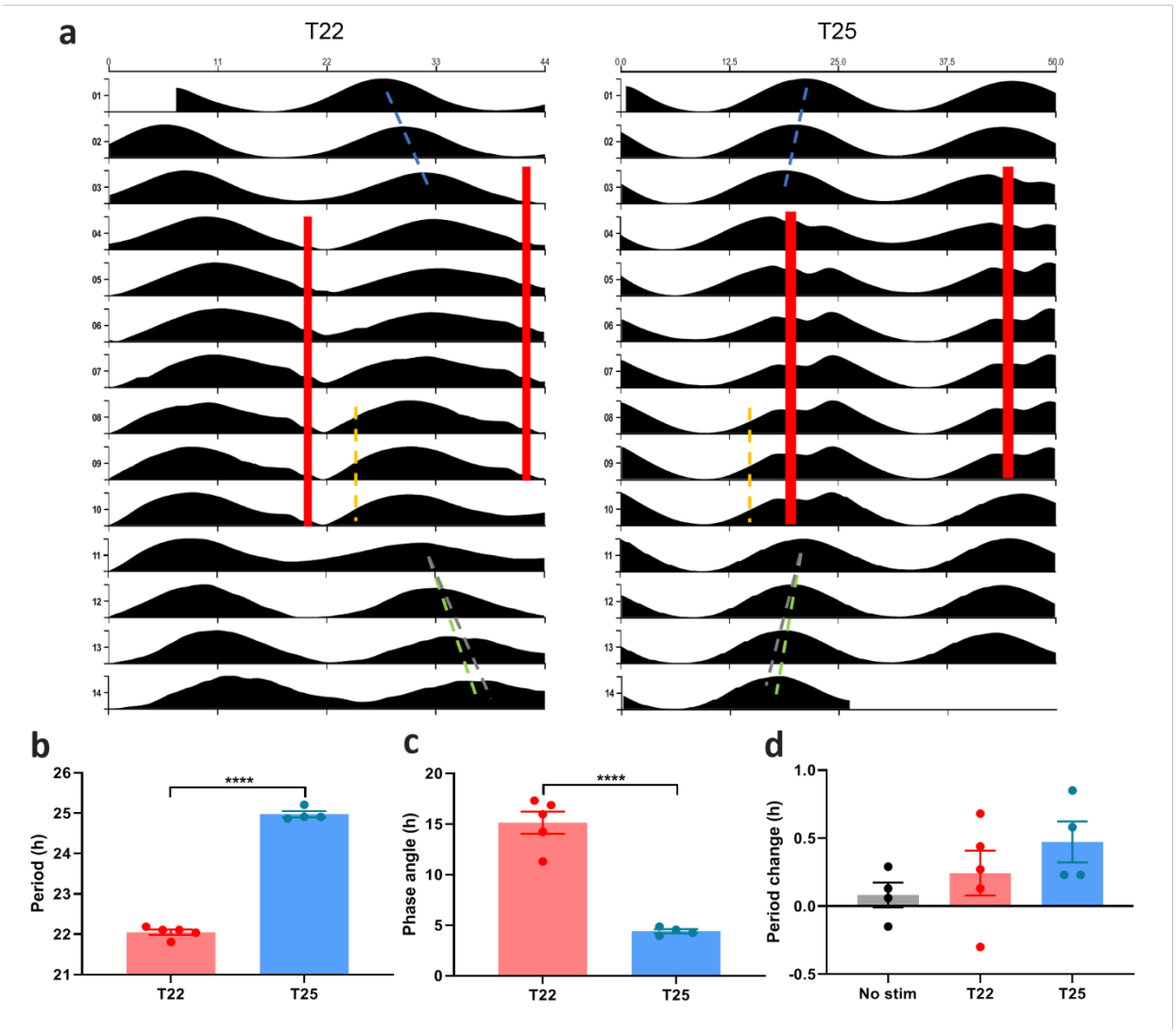

Fig. 3: One-pulse optogenetic T cycle entrainment. a Representative double-plotted PER2::LUC bioluminescence actograms of the SCN slice entrained with 1-1.5h 10Hz optogenetic pulse (red bar) in every 22h (left) or 25h (right). Actograms are depicted in a 22h (left) or 25h (right) format. Linear regressions of the pre- and post-entrainment cycle peaks are indicated as the blue and green dashed lines, respectively. Yellow dashed lines indicate half-maxes of the rising phase during entrainment. Grey dashed lines indicate the pre-entrainment cycle period as a reference. **b-d** Quantification of period during entrainment (**b**), phase angle of entrainment (**c**), period change by entrainment (**d**). **b** and **c** were analyzed using Student t-test (mean ± SEM, n = 4-5, ****$p < 0.0001$), and **d** was analyzed using one-way ANOVA (mean ± SEM, n = 4-5).

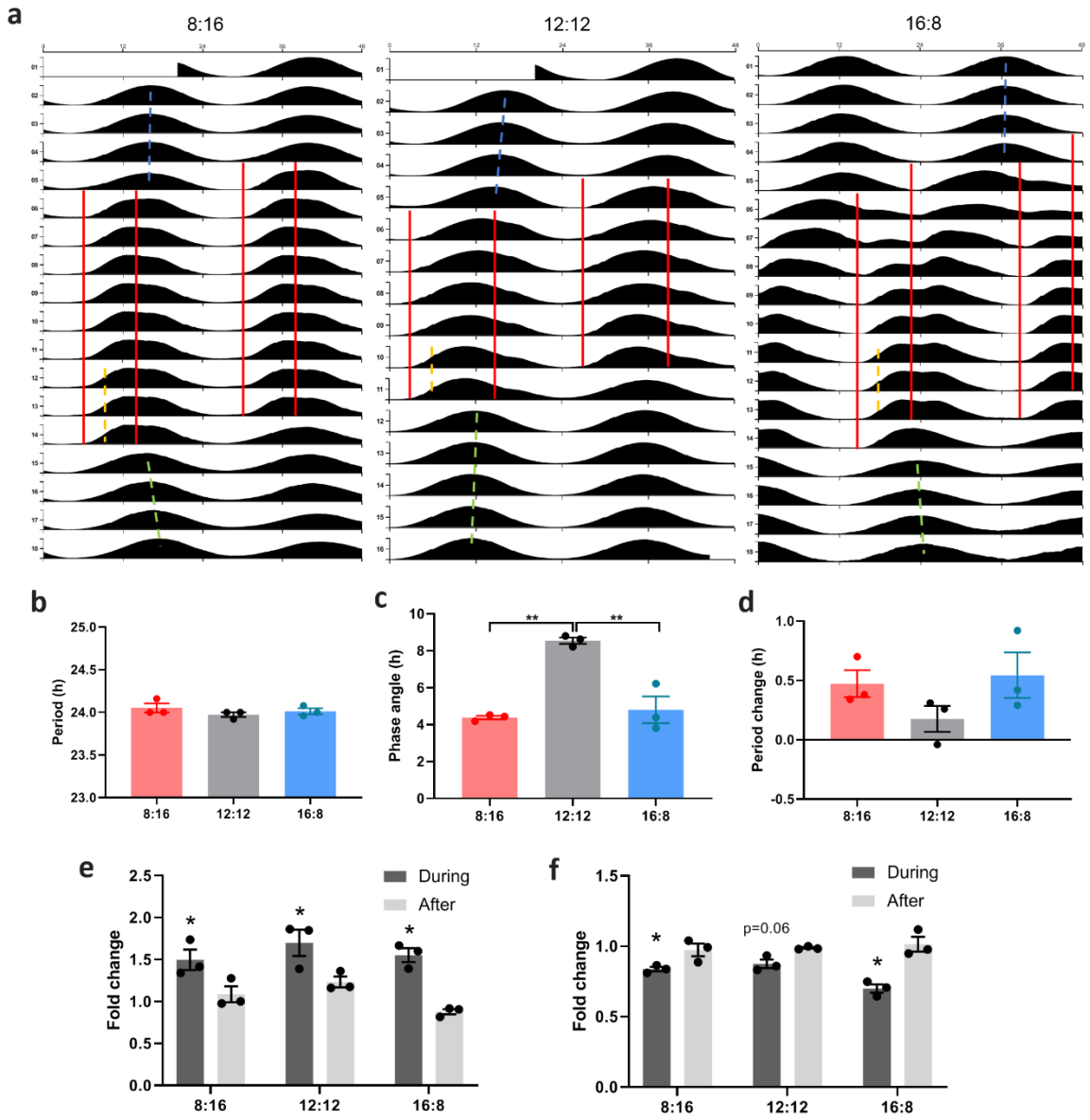

Fig. 4: Optogenetic skeleton photoperiod entrainment. a Representative double-plotted PER2::LUC bioluminescence actograms of SCN slices entrained with 15-min 10Hz red optogenetic pulses (red bars) in 8:16 (left), 12:12 (middle), or 16:8 (right) interval of 24h. For example, 8:16 indicates that the dawn and dusk pulses of the same cycle are given with an 8h interval and the next dawn pulse is given 16h after the dusk pulse of the previous cycle. Linear regressions of the pre-, post-entrainment cycle peaks and during-entrainment cycle half-maxes are indicated as the blue, green, and yellow dashed lines, respectively. **b-d** Quantification of period during entrainment (**b**), phase angle of entrainment (**c**), period change following entrainment (**d**). (One-way ANOVA with Turkey's multiple comparisons test, mean ± SEM, n = 3, **p < 0.01). **e-f** Fold changes in the peak of the rising phase slope **(e)** and in the rising phase duration **(f)** during and after entrainment, compared to before entrainment. (Ratio paired t-test, mean ± SEM, n = 3, *p < 0.05).